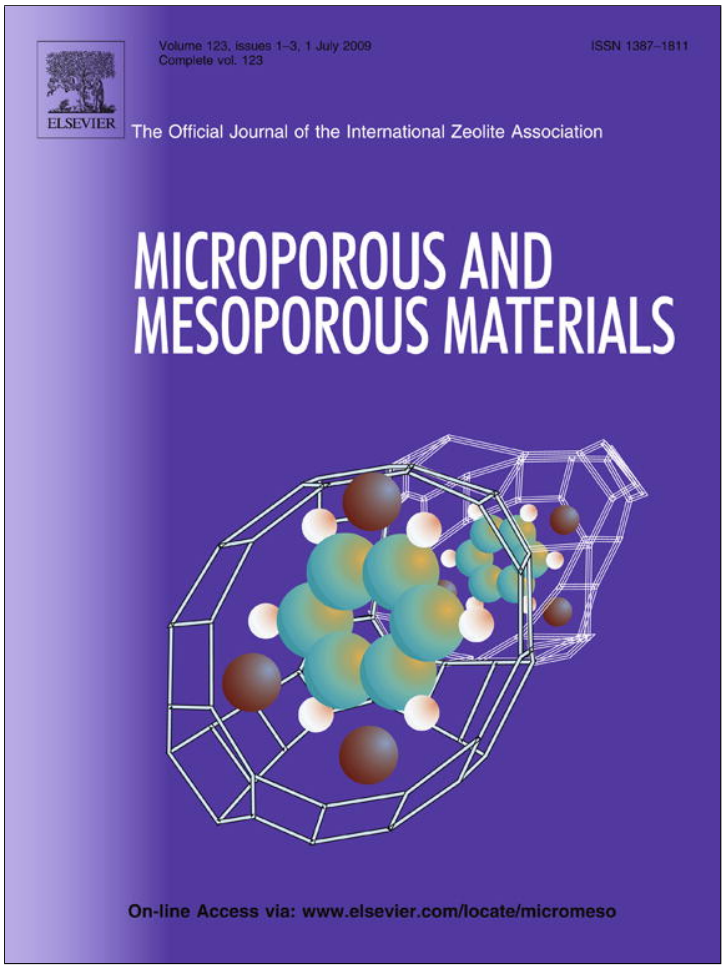

Microporous and Mesoporous Materials 123 (2009) 15–20

Contents lists available at ScienceDirect

Microporous and Mesoporous Materials

journal homepage: www.elsevier.com/locate/micromeso

Mobility of acidic protons in zeolites: A neutron diffraction study of D-heulandite

Annalisa Martucci [a], Ilaria Parodi [a], Petra Simoncic [b], Thomas Armbruster [b], Alberto Alberti [a,*]

[a] Dipartimento di Scienze della Terra, Università di Ferrara, Via G. Saragat, 1, 44100 Ferrara, Italy
[b] Laboratorium für Chemische und Mineralogische Kristallographie, University of Bern, Bern Switzerland

ARTICLE INFO

Article history:
Received 12 January 2009
Received in revised form 9 March 2009
Accepted 10 March 2009
Available online 17 March 2009

Keywords:
Zeolite
Heulandite
Deuterium form
Brønsted acid sites
Neutron powder diffraction
Ion pairs

ABSTRACT

Neutron Rietveld refinement of a natural heulandite (Si/Al = 3.1) in its deuterium form was performed in space group *C*2/*m*. Two Brønsted acid sites were identified. One was on framework oxygen O1, occupied to 20% and headed toward the center of the 8-membered ring channel running parallel to [102]; the other was on O6, occupied to 30% and headed toward the 10-membered ring channel running parallel to the *c*-axis. Three other extraframework sites, located around a distance of 3 Å from the framework oxygens, were attributed to reabsorbed H_2O molecules. On the whole, about 3.2 Brønsted acid sites were located representing about 37% of the value expected on the basis of the aluminium content. This discrepancy is attributed to proton transfer from the Brønsted site to reabsorbed H_2O molecules, forming either a hydroxonium ion (H_3O^+) or charged clusters such as $(H_5O_2)^+$ and $(H_7O_3)^+$.

1. Introduction

Acidic zeolites are widely used in the chemical and petroleum industry because of their catalytic activity, remarkable reaction selectivity, and excellent chemical and thermal stability. Catalytic cracking, heavy oil hydrocracking and methanol to olefin reactions [1] are their most important technological applications. The principal acidity mechanism in these materials is the donation of Brønsted acid protons from bridging framework hydroxyls. Therefore, the location of these hydroxyl groups in acidic zeolites provides a basis for the interpretation of these properties. For this reason, the protonated or deuterated forms of zeolites have long been subject of research. Up to now, investigations on acidic forms of Y [2], Rho [3], SSZ-13 [4], SAPO-34 [5], mordenite [6], ERS-7 [7], ferrierite [8] and SAPO-37 [9] have been carried out by X-ray or neutron diffraction in order to obtain the location and population of Brønsted sites. The use of neutron diffraction on deuterated samples takes an advantage of the fact that ^2H (deuterium) has a large coherent scattering cross-section for neutrons.

The aim of this work is to determine position and concentration of hydroxyl groups in calcined D-heulandite via neutron powder diffraction. The zeolite synthetically modified in this work is well-crystallized heulandite-Ca, $Ca_{3.54}Na_{0.96}K_{0.09}Al_{8.62}Si_{27.51}O_{72}{\cdot}$ca. 20 H_2O obtained from Nasik, India [10,11].

Heulandite-type zeolites are among the most abundant microporous aluminosilicates in nature. According to the Zeolite Subcommittee of the Commission on New Minerals and Mineral Names of the International Mineralogical Association (IMA) two minerals, heulandite and clinoptilolite, have the same topology [IZA code HEU]. Heulandite is defined as the zeolite mineral having an Si/Al ratio <4.0, and clinoptilolite is defined as having an Si/Al ratio $\geqslant$4.0. A suffix indicates the chemical symbol of the most abundant extraframework element, e.g. heulandite-Na, heulandite-Ca, and clinoptilolite-K. [12]. Therefore, the mineral used in this work is classified as heulandite-Ca.

Heulandite-type zeolites can be of a sedimentary or hydrothermal genesis. According to Gottardi and Obradovic [13] a zeolite is considered as sedimentary when it is "a significant constituent of sedimentary rocks (*sensu latu*) ... as long as the zeolite is homogeneously distributed throughout the rock", and is considered as hydrothermal if the zeolite "is clustered in veinlets, geodes or fissures, without any evident reaction with the host rock". The genetic growth environment is important because the dominant part of heulandite-type material applied in technological application is of "sedimentary" origin. Historically the name "clinoptilolite" is associated to sedimentary materials and "heulandite" is associated to the materials of hydrothermal genesis. However, the classification in hydrothermal and sedimentary heulandite-type materials does not match up with the classification in heulandite and clinoptilolite according to the IMA Commission's criterion. Even if the Si/Al ratio is usually less than four in the minerals of hydrothermal genesis and greater than four in the materials crystallized in sedimentary environment, there are clinoptilolites of almost certain hydrothermal origin as well as "sedimentary" heulandites. It is interesting to note that if in addition to Si and Al the most common

* Corresponding author. Tel.: +39 0532 974732; fax: +39 0532 974767.
E-mail address: alb@unife.it (A. Alberti).

1387-1811/$ - see front matter © 2009 Elsevier Inc. All rights reserved.
doi:10.1016/j.micromeso.2009.03.014

extraframework cations (Ca, Na, K, Mg, Sr, Ba) and H_2O molecules are taken into account, discriminant analysis is able to correctly classify ca. 96% of heulandite-type minerals with regard to their genetic groups [14].

The topological symmetry of heulandite-type minerals is $C2/m$ with approximate unit-cell parameters $a = 17.7$ Å, $b = 17.9$ Å, $c = 7.4$ Å, $\beta = 116°$. A two-dimensional channel arrangement parallel to (0 1 0) characterizes the HEU framework. Channels delimited by 10-membered (7.5 × 3.1 Å) and 8-membered (4.6 × 3.6 Å) tetrahedra rings run parallel to the c-axis. These channels are cross-linked by additional eight-ring channels which run parallel to [1 0 0] and [1 0 2]. There is still a doubt about the true symmetry of heulandites and clinoptilolites. $C2/m$ is the maximum symmetry, which may be lowered to $C2$, Cm, $C-1$ and $C1$, due to different Si/Al preferences on tetrahedral sites associated with specific locations of extraframework cations and H_2O molecules [15].

It is known that the behaviour of HEU structures when heated strongly varies as a function of the extraframework cations. In particular natural Ca-dominant [16,17] and Cd^{2+}-exchanged heulandites [18] heated over 250 °C transform into a new phase (usually called phase B) characterized by strong distortion of the framework and breaking of T–O–T bridges with the formation of new T–O–T connections, which partially occlude the 10-membered ring channels. These T–O–T breakings do not occur in K-dominant heulandite [19], in natural Na-, Ca-rich K-poor clinoptilolites [20], and in natural Na-poor Ca-, Mg-, K-rich clinoptilolites [21]. As a general rule, the prevailing presence of small divalent extraframework cations seems to allow the breaking of T–O–T bridges whereas the HEU framework with monovalent extraframework cations preserves its topology upon heating. Therefore, it is highly probable that heating above 250–300 °C causes the breaking of T–O–T bridges in our heulandite-Ca starting sample whereas this phase transformation does not occur in its Na-, NH_4-exchanged or acidic forms. The last assumption will be confirmed by a structure refinement of dehydrated acid heulandite also named D-heulandite.

2. Experimental

2.1. Production of precursor dehydrated heulandite-Na

The starting material was pulverized natural heulandite-Ca obtained from Nasik, India [10]. Ca and other minor extraframework ions were exchanged by Na^+ to obtain a homoionic starting material. Cation exchange was obtained by mixing and stirring the heulandite powder in 2 M NaCl solution. Exchange was first attempted for two weeks at ambient conditions. As this procedure did not yield Na-exchanged heulandite-Na completely, the powder and the exchange solution were placed in a Teflon-coated autoclave at 433 K for additional two weeks. Complete exchange (the absence of Ca and K) was verified by using the energy dispersive system (EDS) of a scanning electron microscope. Heulandite-Na was then filled in a glass ampoule, dehydrated under vacuum (3×10^{-3} mbar) for 24 h at 580 K, and was subsequently sealed.

2.2. Production of precursor heulandite-ND_4

Subsequent treatment of dehydrated heulandite-Na was undertaken in a glove-bag in an argon or nitrogen atmosphere. Dehydrated heulandite-Na was stirred for three weeks at 25 °C in 2 M ND_4Cl solution in D_2O. After a period of 10 days the exchange solution was replaced. Complete ND_4-exchange was verified by EDS analyses (absence of Na) with the scanning electron microscope. Subsequently, the sample was filtered and washed with D_2O.

2.3. Preparation of acidic heulandite

Heulandite-ND_4 was refilled in a glass ampoule and heated under vacuum for 24 h at 770 K to remove D_2O and ND_3. The glass ampoule was sealed under vacuum to avoid contact with air and humidity. Finally, the heat-treated heulandite sample was repacked in an argon-flushed glove-bag from the ampoule into a vanadium container sealed with a rubber gasket and six screws to ensure humidity-free transport to the neutron source.

2.4. Neutron diffraction

Neutron powder patterns were collected at 2.25 K at the D2B line (ILL, Grenoble). Rietveld structure refinements were performed with the GSAS package [22]. The unit-cell parameters of D-heulandite obtained by Rietveld refinement are given in Table 1. The cell volume (2072(1) Å^3) is significantly smaller (2.5%) than that of the NH_4-exchanged form (2126(1) Å^3) and of the untreated heulandite-Na (2107.0(5) Å^3). The main cause of the volume decrease in acid heulandite is related to the decrease in the b parameter. Framework atoms of NH_4-heulandite [23] provided the initial parameters of structure refinement. Extraframework atoms were localized by Fourier maps and were refined by least-squares methods.

Two Brønsted acid sites were located. The position of each deuterium atom was initially restrained geometrically using an O–D distance of 1.00 Å, but these restraints were relaxed in the last cycles of refinement, and both the coordinates and occupancies of the deuterium atom were allowed to refine independently. Details of the refinement are given in Table 1, final atomic positions and occupancies in Table 2, bond distances and angles in Table 3. The final observed and calculated patterns are shown in Fig. 1.

3. Discussion and conclusions

From the structure refinement of the heulandite studied in this work, two Brønsted acid sites were located (see Table 2). The first one, D1, is on framework oxygen O1 pointing toward the center of the 8-membered ring channel running parallel to [1 0 2]; the second one, D2, is on the framework oxygen O6 pointing toward the 10-membered ring channel running parallel the c-axis (see Fig. 2).

The deuterium sites have occupancies of 19% and 31% for D1 and D2, respectively. The two Brønsted groups show quite regular site geometry (see Fig. 3).

The most remarkable difference with respect to the framework of the NH_4-exchanged heulandite [23] is observed in the T2–O1–T2 angle related to the D1 site, which is narrow in the dehydrated acid

Table 1
Lattice parameters and refinement details for D-heulandite.

Space group	$C2/m$
a (Å)	17.662(2)
b (Å)	17.713(2)
c (Å)	7.416(1)
$\beta°$	116.7(1)
V (Å)^3	2072.3(5)
Refined pattern min/max 2θ (°)	10–120
R_{wp} (%)	4.38
R_p (%)	3.43
R_F^2 (%)	8.5
N_{obs}	2810
N_{var}	105

Notes: Neutron radiation, $\lambda = 2.39845(1)$ Å.
$R_p = \sum[Y_{io} - Y_{ic}] / \sum Y_{io}$; $R_{wp} = [w_i(Y_{io} - Y_{ic})^2 / \sum w_i Y_{io}^2]^{0.5}$.
$R_F^2 = \sum |F_0^2 - F_c^2| / \sum |F_0^2|$.
Estimated standard deviations in parentheses refer to the last digit.

Table 2
Atomic coordinates, thermal parameters and site occupancies of framework atoms for D-heulandite.

Atom	*x*/*a*	*y*/*b*	*z*/*c*	Fraction	U_{iso}
T1	0.1813(3)	0.3336(4)	0.0982(5)	1.000	0.002(1)
T2	0.2861(4)	0.4153(4)	0.4902(6)	1.000	0.002(1)
T3	0.2845(5)	0.1850(4)	0.2785(7)	1.000	0.002(1)
T4	0.4295(5)	0.2975(5)	0.5748(7)	1.000	0.002(1)
T5	0	0.2891(6)	0	1.000	0.002(1)
O1	0.3236(6)	0.5	0.5560(9)	1.000	0.004(1)
O2	0.2591(6)	0.1119(8)	0.3721(11)	1.000	0.004(1)
O3	0.3050(6)	0.1512(6)	0.1013(10)	1.000	0.004(1)
O4	0.2308(5)	0.4029(7)	0.2485(9)	1.000	0.004(1)
O5	0.5	0.3202(9)	0.5	1.000	0.004(1)
O6	0.0805(7)	0.3416(7)	0.0319(10)	1.000	0.004(1)
O7	0.3667(6)	0.2298(4)	0.4440(11)	1.000	0.004(1)
O8	0.0248(5)	0.2355(7)	0.1964(9)	1.000	0.004(1)
O9	0.2104(7)	0.2465(8)	0.1602(10)	1.000	0.004(1)
O10	0.3769(6)	0.3756(5)	0.5450(9)	1.000	0.004(1)
X1	0.210(2)	0	0.011(4)	0.989(5)	0.034(2)
X2	0.001(2)	0	0.612(2)	0.500(5)	0.092(2)
X3	0.154(3)	0.5	0.918(4)	0.550(5)	0.081(2)
D1	0.156(2)	0	0.550(4)	0.191(5)	0.019(3)
D2	0.042(3)	0.396(4)	0.017(4)	0.307(3)	0.008(3)

Note: estimated standard deviations in parentheses refer to the last digit. Isotropic displacement factors U_{iso} fixed for T and O atoms, respectively. Occupancy of the T sites: Si = 76% , Al = 24%.

Table 3
Selected bond distances (Å) and angles (°) within the framework of D-heulandite.

T1–O3	1.625(8)	T2–O1	1.624(8)	T3–O2	1.625(14)
T1–O4	1.624(12)	T2–O2	1.626(11)	T3–O3	1.626(10)
T1–O6	1.626(12)	T2–O4	1.625(8)	T3–O7	1.626(11)
T1–O9	1.626(15)	T2–O10	1.627(12)	T3–O9	1.624(14)
T4–O5	1.625(9)	T5–O6 [x2]	1.625(13)	D2–O6	1.16(7)
T4–O7	1.626(11)	T5–O8 [x2]	1.625(11)	D1–O1	1.00(3)
T4–O8	1.625(9)				
T4-O10	1.625(13)				
X1–O2 [x2]	3.12(2)	X2–O1	2.97(3)	X3–O3 [x2]	2.79(2)
X1–O3 [x2]	3.07(2)	X2–O5 [x2]	3.29(2)	X3–O4 [x2]	2.80(2)
X1–O4 [x2]	3.09(3)	X2–O10 [x2]	2.99(2)	X3–X1	2.22(6)
X1–X3	2.22(6)	X2-X2	1.65(3)		
T2–O1–T2	135.0(7)	T1–O6–T5	139.6(9)		
T2–O2–T3	144.3(9)	T3–O7–T4	161.6(7)		
T1–O3–T3	148.5(8)	T4–O8–T5	162.4(8)		
T1–O4–T2	136.9(8)	T1–O9–T3	149.9(9)		
T4–O5–T4	151.3(12)	T2–O10–T4	147.3(7)		

Note: estimated standard deviations in parentheses refer to the last digit.

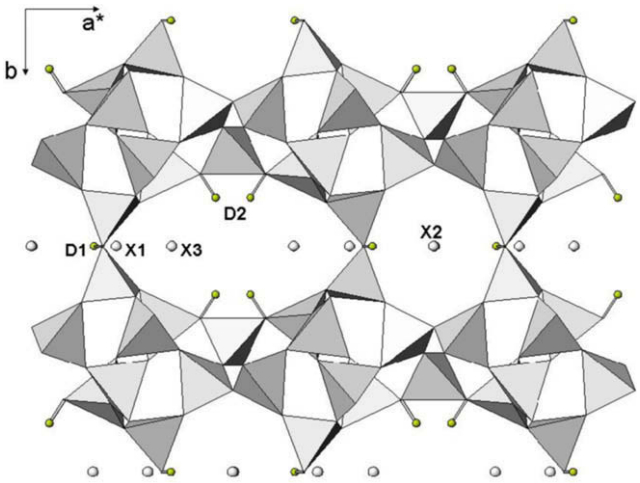

Fig. 2. Location of Brønsted (D) and water molecule (X) sites in D-heulandite viewed down the [001] direction.

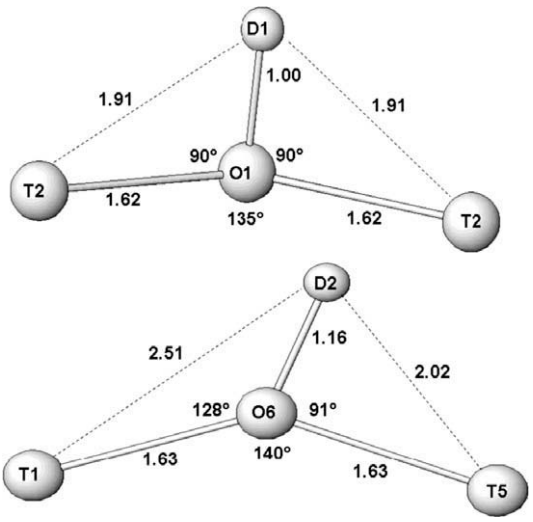

Fig. 3. Geometry of D1 (top) and D2 (bottom) Brønsted acid sites.

phase, but significantly larger in NH_4-exchanged heulandite (135° and 153°, respectively; see Table 3). It is known that if a Brønsted

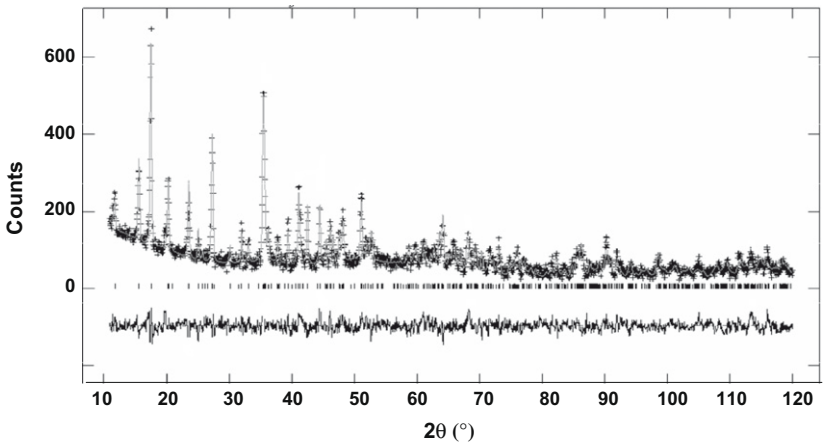

Fig. 1. The neutron diffraction observed (crossed) calculated (continuous line), and difference (bottom line) profiles of D-heulandite.

proton forms an hydroxyl group the related T–O–T angle usually narrows [24], therefore, this result confirms that O1 becomes a Brønsted acid site. On the whole, about 3.2 acid sites were located in the unit cell, corresponding to only 37% of the measured aluminium content and the associated NH_4 content necessary for charge balance in the hydrated NH_4 phase [23].

Thus the refined concentration of Brønsted acid sites is considerably lower than expected, but this result is in line with findings by many authors. Bankós et al. [25], Crocker et al. [26], Datka et al. [27], Sawa et al. [28] and Rodriguez-Gonzales et al. [29] showed that for zeolites with high Al content the concentration of Brønsted sites is remarkably lower than predicted from the aluminium content. In particular, Sonnemans et al. [30] demonstrated that there is a significant nonlinear deviation between the actual concentration on the one hand and the possible maximal concentration of Brønsted sites on the other hand. This discrepancy increases with increasing Al content. According to their results, the experimentally determined Brønsted sites for an Si/Al ratio as low as 3.1, as is the case of our sample, may not account for up to 70% of the theoretical value. A number of reasons, such as an incomplete NH_4^+ ion exchange, dehydroxylation and/or dealumination occurring during calcination, as well as residual NH_4^+ after calcination, have been put forward to explain the lower concentration of Brønsted acid sites [30]; this point will be discussed later.

In the present work, three additional extraframework sites (X1, X2 and X3 in Tables 2 and 3 and Fig. 1) were recognized in D-heulandite, all at long distances from the framework. Some hypotheses can be suggested about their nature:

(a) The extraframework sites may represent residual Na cations due to an incomplete NH_4^+ ion exchange. This hypothesis is highly improbable as a chemical (EDS) analysis was performed on the studied material after NH_4-exchange. In addition, single crystals used to study the crystal structure of NH_4-exchanged heulandite [23] also indicated a complete cation exchange Na → NH_4.

(b) The extraframework sites may represent residual ND_4 groups after calcination. Difference Fourier synthesis does not show any indication of positive maxima at about 1 Å from these sites, attributable to D atoms of ND_4 groups or D_2O molecules; this fact together with the long duration (24 h under vacuum) and high temperature treatment (770 K) excludes that there is residual D_2O or ND_4 after calcination. As a result, the presence of a significant residue of ND_4 or D_2O in the D-heulandite samples studied seems improbable and may be disregarded.

(c) The extraframework sites may represent extraframework Al atoms caused by dealumination of the framework. Firstly, the procedure followed to obtain D-heulandite should avoid significant dealumination of the framework. Moreover, the Rietveld difference Fourier synthesis does not show any maximum, which can be interpreted as oxygen atoms coordinated to hypothetical extraframework Al. As a consequence we may exclude dehydroxylation due to dealumination of the framework. We may also exclude dehydroxylation associated with a significant amount of three-coordinated framework aluminium as the structure refinement does not show any remarkable distortion of the tetrahedral framework. It should also be noted that only 3.2 Brønsted acid sites have been localized compared with 8.8 Al atoms given by the chemical analysis and such a high number of tetrahedral defects should be evidenced by the structure refinement.

(d) The location of the extraframework site X1 is intermediate between that of fully occupied N3 found in NH_4-exchanged heulandite [23] and of a H_2O site (frequently called W1) found in natural and cation-exchanged heulandite–clinoptilolite minerals, which is usually the H_2O site with highest occupancy. All three sites, X1, W1, N3 are 6-fold coordinated and bonded to the same framework oxygens, and 2-fold coordinated to O2, O3 and O4, respectively (see Fig. 4). As far the X2 and X3 sites are concerned, their position does not resemble those of other extraframework sites found in other structures with HEU topology. The distance X2–X2 (see Table 3) too short for the simultaneous occupation of both sites is justified by the partial occupancy of X2. It should also be noted that the use of nitrogen or oxygen scattering cross-sections for neutrons does not remarkably influence the occupancy of X1, X2, and X3 sites found in the diffraction experiment. The absence of maxima attributable to deuterium atoms located near these sites supports the hypothesis that the additional extraframework sites may represent re-adsorbed H_2O molecules. We may speculate leaking when the ampoule was melted off after calcinations under vacuum or there was significant humidity when the sample was filled into the vanadium cylinder for neutron data collection. In such case X1, X2, and X3 represent about 40% of the H_2O molecules found in the single-crystal structure refinement of hydrated NH_4-exchanged heulandite [23]. This fraction seems very high but we have to consider the strongly hydrophilic behaviour of the heulandite powder sample due to the low Si/Al ratio (3.1). We must also consider that a considerable portion of extraframework space is occupied by ammonium ions in NH_4-exchanged heulandites but the corresponding space is empty in D-heulandite and may be filled with additional H_2O molecules.

(e) Once the presence of significant residual NH_4^+ ions or extraframework Al atoms is disregarded, another explanation must be found to justify the experimental evidence that the concentration of Brønsted sites is by far lower than the theoretical value given by the Al content. On the other hand it is highly improbable that the high discrepancy between expected and analysed D sites is an artefact due to underestimation of the acid sites in our structure refinement. The ability of Brønsted acid sites to react with adsorbed H_2O molecules to form hydroxonium ions, H_3O^+, has been studied by many authors by means of a variety of experimental techniques and computational methodologies. The formation of hydroxonium ions has been envisaged for many years (e.g. [31]) but still today unambiguous evidence of their presence has not yet been adduced. Infrared spectra obtained for samples with a loading level of one H_2O molecule per Brønsted site have been interpreted as due to the formation of a hydroxonium ion [32] or a neutral

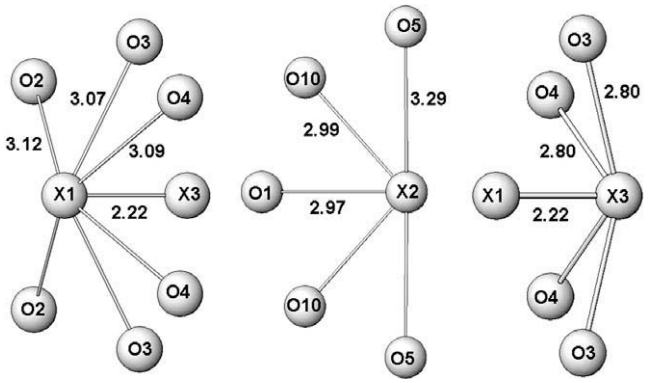

Fig. 4. Coordination of water molecule sites.

hydrogen-bonded complex [33] or to the simultaneous presence of both species [5,34] or to the presence of $H_5O_2^+$ or $H_7O_3^+$ clusters [35,36]. The effect of H_2O molecules adsorbed on bridging hydroxyl groups has also been studied by ^1H MAS NMR measurements [37,38]. The results indicate the simultaneous presence of hydroxonium ions and hydrogen-bonded H_2O up to a level of one H_2O molecule per Brønsted site. Moreover the shift of the ^1H NMR of bridging OH groups can be interpreted by fast proton exchange between H_2O molecules, bridging OH groups and hydroxonium ions [37]. In H-mordenite after water adsorption, the observed vibrational features in neutron inelastic scattering experiments are assigned to hydroxonium ions, hydrogen-bonded H_2O, and free hydroxyl groups. Stuckenschmidt et al. [39] detected the presence of H_3O^+ groups in calcined and re-hydrated ammonium-natrolite by using single-crystal X-ray diffraction data. Many computational studies have been performed in order to study the interaction of H_2O molecules with acid centres in H-zeolites. These calculations seem to indicate that with one H_2O molecule per acid site the structure is energetically stabilized, while the hydroxonium ions correspond to a transition state for proton exchange. At higher coverage (two or more molecules per acid site) protonated complexes are stabilized [40–42]. The calculated low proton affinity of H_2O (694 kJ mol^{-1}) and the by far larger proton affinity of H_2O dimers and trimers (806 and 853 kJ mol^{-1}), which can be compared with that of ammonia (858 kJ mol^{-1}) [43], which is always protonated in any H-zeolite, are seen as obstacles to the protonation of single H_2O molecules in H-zeolites but not to the protonation of H_2O dimers and trimers [36]. In contrast, molecular dynamic simulations of H_2O molecules adsorbed in gmelinite [44] and mordenite [45] indicate that even a single H_2O is sufficient to produce a hydroxonium ion.

In conclusion, experimental results and computational studies provide convincing evidence for proton transfer from the Brønsted site to reabsorbed H_2O molecule, forming either a hydroxonium ion (H_3O^+) or charged clusters such as $(H_5O_2)^+$ and $(H_7O_3)^+$. The latter interpretation is favoured by computational approaches (e.g., [36] and references therein).

As reported before, three potential H_2O sites, summing up to ca. 7.5 molecules per unit cell, were determined in D-heulandite; one of these (X2) is at coordination distance (see Table 3) only to framework oxygens. X1 and X3 are also coordinated by framework oxygens but are linked to H_2O dimers with the distance X1–X3 = 2.22 Å (Table 3). This distance seems quite short for an Ow–Ow separation but the standard error is large. Computational studies gave for a H_2O–H–OH_2 cluster an ideal Ow–Ow distance around 2.4 Å, where equal OH distances indicate the formation of a protonated water dimer [43]. Moreover, experimental finding by neutron powder diffraction indicates that the average oxygen–oxygen distance in a DO···D···OD dihydroxide anion in deuterated sodalite is as short as 2.28 Å [46]. Therefore, we assume that the discrepancy between the experimentally found Brønsted acid sites and their theoretical value (based on framework Al) is explained by the presence of hydroxonium ions or charged H_2O clusters.

However, Sonnemans et al. [30] showed that there is a significant nonlinear deviation between the concentration of Brønsted acid sites, determined by conductometric titration and infrared spectroscopy, and the theoretical concentration expected on the basis of the aluminium content. The lower the Si/Al ratio, the higher the discrepancy. These authors attributed this discrepancy to dealumination and dehydroxylation processes occurring during calcinations and proposed a model according to which the degree of these processes strongly depends on the concentration of paired Brønsted acid sites, which in turn is related to the concentration of vicinal tetrahedral aluminium sites in the zeolite framework.

A similar mechanism was invoked by Marosi [47]; dehydroxylation occurs in two steps: in the first step H_2O is eliminated from those hydroxyl groups which are coordinated to neighbouring framework aluminium atoms thus forming three-coordinated framework Al. The second step of dehydroxylation always involves the migration of framework aluminium ions into the extraframework pore system. With these interpretations dehydroxylation strongly depends on the Si/Al ratio.

According to our hypothesis, dehydroxylation is still related to the Al fraction in the tetrahedral framework but the mechanism of dehydroxylation is completely different. It is well known that the hydrophilicity or hydrophobicity of a zeolite depends on its Si/Al ratio. Usually the NH_4-exchanged zeolite is heated to obtain its acid form and the sample is subsequently placed on the instrumental holder (vanadium container). During this operation the sample must have been partly rehydrated, even if the relocation was fast, scrupulous and performed under cover gas to reduce humidity. The amount of reabsorbed H_2O is roughly a function not only of the time lapsed during refilling but also of the sample hydrophilicity, i.e. its Si/Al ratio.

In dehydrated H-SSZ-13 (CHA topology) [4] where the Si/Al ratio is 16, no detectable amount of H_2O was evidenced, and the concentration of Brønsted acid sites corresponded to the theoretical value. The presence of a hydroxonium ion has been observed in the hydrated form of SSZ-13 through infrared spectroscopy. It is interesting to note that in H-SSZ-13 Brønsted sites were localized on the framework oxygens O1 and O2 whereas in H-SAPO-34 (CHA topology) [5] protonation was observed at oxygens O2 and O4. However, with low H_2O loading in H-SAPO-34 the proton was removed from O4 to form a hydroxonium ion interacting with O1. In D-ERS-7 (IZA code ESV) [7] the Si/Al ratio was 8.3, 65% of the theoretical concentration of acid sites was found and no other extraframework sites were reported. In synthetic ferrierite [8] the Si/Al ratio was 8.5, 2.4 hydroxyl groups (63% of the amount assumed from Al atoms) and 1.9 H_2O molecules were found in the unit cell. Three samples of mordenite [6] with an Si/Al ratio of 5.5, 5.6 and 10.0, respectively, were studied. 2.8, 2.4 and 2.4 H_2O molecules and 3.2, 3.5 and 2.8 Brønsted sites (44%, 48% and 64%, respectively, of Al atoms) were localized in the unit cell. An interesting feature was found in D–Y zeolite [2]. In the dehydrated sample (Si/Al = 2.43), three hydroxyl groups were found, accounting for about 90% of the (Al–Na) content. When the sample was slightly rehydrated (about 15 H_2O molecules compared to 384 framework oxygens) the deuterons of one of the hydroxyl groups (accounting for about 40% of the deuterons found in the dehydrated sample) shifted in the direction of an H_2O molecule up to a distance of 1.16 Å from the oxygen of the molecule while the distance to the framework oxygen increased up to 2.04 Å. The authors interpreted this shift as the jump of the deuterons to the H_2O molecules with the formation of hydroxonium ions.

Many authors have tackled the problem of the proton jump energy barrier by density functional theory (DFT) calculations. The calculated barriers for on-site proton jump vary within the range 60–100 kJ mol^{-1} for CHA, FAU and MFI structures [48,49], whereas the proton jump barriers experimentally determined by ^1H NMR technique are significantly lower than the calculated ones (around 15–25 kJ mol^{-1}) [49,50]. This discrepancy has been explained by the presence of undetected H_2O in the sample [51]. It is therefore evident that the presence of H_2O favours the proton transfer from the Brønsted acid sites to H_2O molecules, thus supporting our hypothesis for the interpretation of the discrepancy between experimentally determined and theoretical hydroxyl groups in acid zeolites.

Acknowledgements

AM, IP, and AA acknowledge the Italian MURST for financial support under the project PRIN 2006 "Zeolites at non-ambient conditions: theoretical–experimental characterization and novel technological applications".

References

[1] A. Corma, Chem. Rev. 95 (1995) 559.
[2] M. Czjzek, H. Jobic, A.N. Fitch, T. Vogt, J. Phys. Chem. 96 (1992) 1535.
[3] R.X. Fischer, W.H. Baur, R.D. Shannon, R.H. Staley, L. Abrams, A.J. Vega, J.D. Jorgensen, Acta Crystallogr. B 44 (1988) 321.
[4] L.J. Smith, A. Davidson, A.K. Cheetham, Catal. Lett. 49 (1997) 143.
[5] L.J. Smith, A.K. Cheetham, R.E. Morris, L. Marchese, J.M. Thomas, P.A. Wright, J. Chen, Science 271 (1996) 799.
[6] A. Martucci, G. Cruciani, A. Alberti, C. Ritter, P. Ciambelli, M. Rapacciuolo, Micropor. Mesopor. Mater. 35–36 (2000) 405.
[7] B.J. Campbell, A.K. Cheetham, T. Vogt, L. Carluccio, W.O. Parker Jr., C. Flego, R. Millini, J. Phys. Chem. B 105 (2001) 1947.
[8] A. Martucci, A. Alberti, G. Cruciani, P. Radaelli, P. Ciambelli, M. Rapacciuolo, Micropor. Mesopor. Mater. 30 (1999) 95.
[9] L.M. Bull, A.K. Cheetham, P.D. Hopkins, B.M. Powell, J. Chem. Soc. Chem. Commun. 1993 (1993) 1196.
[10] R.N. Sukheswala, R.K. Avasia, M. Gangopadhyay, Mineral. Mag. 39 (1974) 658.
[11] P. Yang, T. Armbruster, J. Solid State Chem. 123 (1996) 140.
[12] D.S. Coombs, A. Alberti, T. Armbruster, G. Artioli, C. Colella, E. Galli, J.D. Grice, F. Liebau, J.A. Mandarino, H. Minato, E.H. Nickel, E. Passaglia, D.R. Peacor, S. Quartieri, R. Rinaldi, M. Ross, R.A. Sheppard, E. Tillmanns, G. Vezzalini, Eur. J. Mineral. 10 (1998) 1037.
[13] G. Gottardi, J. Obradovic, Fortschr. Mineral. 56 (1978) 316.
[14] A. Alberti, M.F. Brigatti, Am. Mineral. 70 (1985) 805.
[15] T. Armbruster, in: A. Galarnau, F. Di Renzo, F. Faujula, J. Vedrine (Eds.), Zeolites and Mesoporous Materials at the Dawn of the 21st Century, Elsevier, Amsterdam, 2001, p. 13.
[16] A. Alberti, G. Vezzalini, TMPM Tschermaks Mineral. Petrograph. Mitt. 31 (1983) 259.
[17] T.M. Khobaer, T. Kuribayashi, K. Komatsu, Y. Kudoh, J. Mineral. Petrolog. Sci. 103 (2008) 61.
[18] N. Doebelin, T. Armbruster, Micropor. Mesopor. Mater. 61 (2003) 85.
[19] E. Galli, G. Gottardi, H. Mayer, A. Preisinger, E. Passaglia, Acta Cryst. B 39 (1983) 189.
[20] T. Armbruster, M.E. Gunter, Am. Mineral. 76 (1991) 1872.
[21] T. Armbruster, Am. Mineral. 78 (1993) 260.
[22] A.C. Larson, R.B. von Dreele, Report LAUR, 86-784, 1994.
[23] P. Yang, T. Armbruster, Eur. J. Mineral. 10 (1998) 461.
[24] J. Sauer, C.M. Kolmel, I.R. Hill, R. Ahlrichs, Chem. Phys. Lett. 164 (1989) 193.
[25] I. Bankós, J. Valyon, G.I. Kapustin, D. Kalló, A.L. Klyachko, T.R. Brueva, Zeolites 8 (1988) 189.
[26] M. Crocker, R.H.M. Herold, M.H.W. Sonnemans, C.A. Emels, A.E. Wilson, J.N. van der Moolen, J. Phys. Chem. 97 (1993) 432.
[27] J. Datka, B. Gil, A. Kubacka, Zeolites 15 (1995) 501.
[28] M. Sawa, M. Niwa, Y. Murakami, Zeolites 10 (1990) 532.
[29] L. Rodriguez-Gonzales, F. Hermes, M. Bertmer, E. Rodriguez-Castellon, A. Jimenez-Lopez, U. Simon, Appl. Catal. A 328 (2007) 174.
[30] M.H.W. Sonnemans, C. den Heejer, M. Crocker, J. Phys. Chem. 97 (1993) 440.
[31] R.M. Barrer, J.J. Klinowski, J. Chem. Soc. Faraday Trans. 1 (71) (1975) 690.
[32] L. Marchese, J. Chen, P.A. Wright, J.M. Thomas, J. Phys. Chem. 97 (1993) 8109.
[33] F. Wakabayashi, J.N. Kondo, K. Domen, C. Hirose, J. Phys. Chem. 100 (1996) 1442.
[34] L. Parker, D.M. Bibby, G.R. Burns, Zeolites 13 (1993) 107.
[35] A. Jentys, G. Warecka, M. Derewinski, J.A. Lercher, J. Phys. Chem. 93 (1989) 4837.
[36] P.W. Kletnieks, J.O. Ehresmann, J.B. Nicholas, J.F. Haw, Chem. Phys. Chem. 7 (2006) 114.
[37] M. Hunger, D. Freude, H. Pfeifer, J. Chem. Soc. Faraday Trans. 87 (1991) 657.
[38] P. Batamack, C. Dorémieux-Morin, R. Vincent, J. Fraissard, J. Phys. Chem. 97 (1993) 9779.
[39] E. Stuckenschmidt, W. Joswig, W.H. Baur, Eur. J. Mineral. 8 (1996) 85.
[40] E. Nusterer, P.E. Blöchl, K. Schwarz, Chem. Phys. Lett. 253 (1996) 448.
[41] S.A. Zygmunt, L.A. Curtiss, L.E. Iton, M.K. Erhardt, J. Phys. Chem. 100 (1996) 6663.
[42] Y. Jeanvoine, J.G. Ángyán, G. Kresse, J. Hafner, J. Phys. Chem. B 102 (1998) 7307.
[43] J. Sauer, in: J.T. Hynes, J.P. Klinman, H.H. Limbach, R.L. Schowen (Eds.), Hydrogen-transfer Reactions, Wiley-VCH, 2007, pp. 685–707.
[44] L. Benco, Th. Demuth, L. Hafner, F. Hutschka, Chem. Phys. Lett. 324 (2000) 373.
[45] Th. Demuth, L. Benco, L. Hafner, H. Toulhoat, Int. J. Quantum Chem. 84 (2001) 110.
[46] M. Wiebcke, G. Engelhardt, J. Felsche, P.B. Kempa, P. Sieger, J. Schefer, P. Fischer, J. Phys. Chem. 96 (1992) 392.
[47] L. Marosi, Angew. Chem. Int. Ed. Engl. 19 (1980) 743.
[48] J.T. Fermann, C. Blanco, S. Auerbach, J. Chem. Phys. 112 (2000) 6779.
[49] C. Tuma, J. Sauer, Chem. Phys. Lett. 387 (2004) 388.
[50] T. Baba, N. Komatsu, Y. Ono, H. Sagisawa, J. Phys. Chem. B 102 (1998) 804.
[51] J.A. Ryder, A.K. Chakraborty, A.T. Bell, J. Phys. Chem. B 104 (2000) 6998.